nature sustainability

Article

https://doi.org/10.1038/s41893-025-01559-z

Natural rubber with high resistance to crack growth

Received: 15 July 2024

Accepted: 2 April 2025

Published online: 07 May 2025

Check for updates

Guodong Nian[1,5], Zheqi Chen[1,2,5], Xianyang Bao[1,5], Matthew Wei Ming Tan[1,3], Yakov Kutsovsky[4] & Zhigang Suo[1]

Natural rubber, with annual production of 15 million tonnes, is the most used bio-elastomer. Improving its resistance to crack growth is highly desired, to prolong its service life for many applications and eventually improve its sustainability. Here we markedly amplify the resistance to crack growth in natural rubber by forming a tanglemer, a polymer network in which entanglements greatly outnumber crosslinks. Specifically, we cast natural rubber latex without high-intensity processing that cuts long polymers. The long polymers densely entangle by thermal motion and are then sparsely crosslinked. At a crack tip, long polymer strands between neighbouring crosslinks deconcentrate stress, extend strain-induced crystallization over a large region and enhance crystallinity. For example, when the ratio of crosslinks to repeat units reduces from 10^{-2} to 10^{-3}, the network amplifies fatigue threshold from ~50 J m^{-2} to ~200 J m^{-2}, and toughness from ~10^4 J m^{-2} to over 10^5 J m^{-2}. Overall, this work provides a viable strategy to improve the practical applicability of natural rubber, contributing to the development of sustainable polymers.

A powerful strategy to develop materials for sustainability is to reimagine the existing economically important materials. Examples include steel[1], glass[2], plastics[3] and concrete[4]. Redesigning biopolymers for improved performance can extend their service life and thus enhance their sustainability. Natural rubber has long been used in high-volume, high-severity applications, such as tyres, belts and hoses. Derived from the *Hevea Brasiliensis* tree, the latex contains natural rubber of long chains and highly regular *cis*-configuration[5]. Both features are critical to the superior performance of natural rubber and have never been fully replicated in its synthetic counterpart. Furthermore, the performance of natural rubber is degraded by commonly adopted processes[6]. The latex is usually dried to form blocks of polymer, which are then mixed with additives in machines such as internal mixers, extruders and roll mills. Such an intense mixing process homogenizes the mixture and lowers its viscosity for shaping the final products. The intense mixing processes masticate the polymers into short chains, which require dense crosslinks to form a network. We call such a network a regular network (Fig. 1a). At a crack tip in the network, stress is deconcentrated over a polymer strand between neighbouring crosslinks, while strain-induced crystallization (SIC) extends to a volume larger than individual polymer strands. The former gives a fatigue threshold of ~40 J m^{-2} (ref. 7) and the synergy of the former and the latter gives a toughness of ~10^4 J m^{-2} (ref. 8).

Here we amplify both fatigue threshold and toughness by processing latex without mastication, letting the long polymer chains form a tanglemer, a polymer network in which entanglements greatly outnumber crosslinks (Fig. 1b). At a crack tip in the tanglemer, stress deconcentrates over a long polymer strand between neighbouring crosslinks. The entanglements function as slip links and do not impede stress deconcentration, thus decoupling modulus and fatigue threshold. The long polymer strands enlarge the volume of SIC and increase the degree of crystallinity. The long polymer strands amplify fatigue threshold to ~200 J m^{-2} and the synergy of the long polymer strands and the SIC amplifies toughness to over 10^5 J m^{-2}. The natural rubber tanglemers greatly outperform existing rubbers (Fig. 1c) and hold promise to extend the lifetimes of established products and to result

[1]John A. Paulson School of Engineering and Applied Sciences, Harvard University, Cambridge, MA, USA. [2]College of Chemical and Biological Engineering, Zhejiang University, Hangzhou, China. [3]School of Materials Science and Engineering, Nanyang Technological University, Singapore, Singapore. [4]Expert-in-Residence, Office of Technology Development, Harvard University, Cambridge, MA, USA. [5]These authors contributed equally: Guodong Nian, Zheqi Chen, Xianyang Bao. e-mail: suo@seas.harvard.edu

https://doi.org/10.1038/s41893-025-01559-z

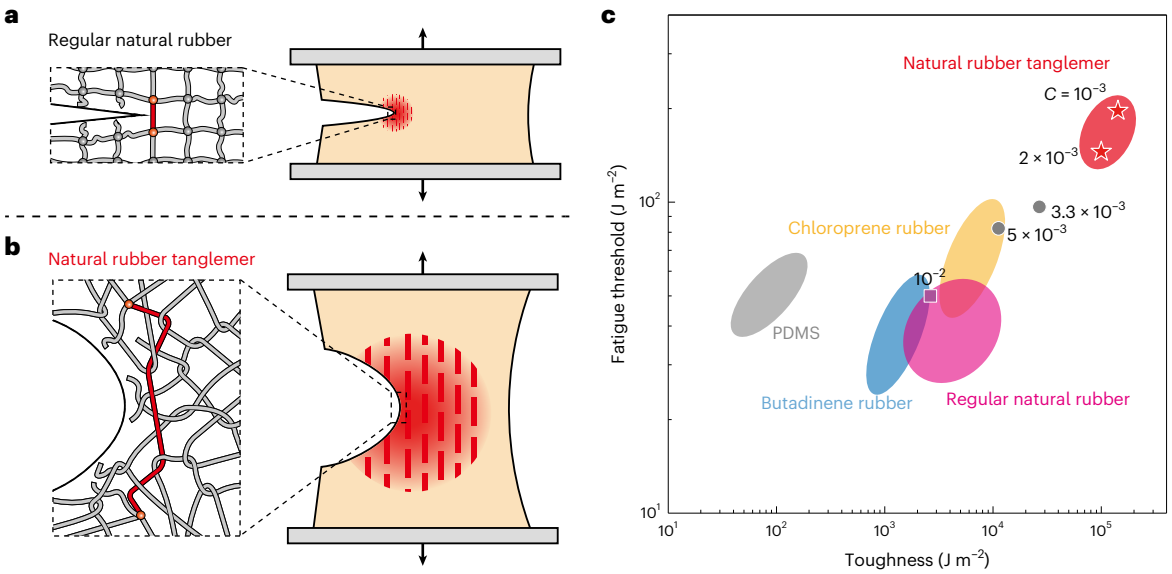

Fig. 1 | Natural rubber tanglemer outperforms regular natural rubber. **a**–**c**, Crosslink density C is defined by the molar ratio of crosslinks to the repeat units of the polymer; toughness and fatigue threshold both increase as the crosslink density decreases. In regular natural rubber ($C \approx 10^{-2}$), a short polymer strand at a crack tip deconcentrates stress over a short distance, while SIC extends to a small volume (**a**). In a natural rubber tanglemer ($C \approx 10^{-3}$), a long polymer strand at a crack tip deconcentrates stress over a long distance, while SIC extends to a large volume (**b**). Various polymer networks are compared in the plane of toughness and fatigue threshold (**c**)[7,8,60,61].

in new products. A more durable biopolymer will reduce polymer pollution and enhance sustainability.

Results

Network design and process

Entangled polymer networks have been studied for decades[9–11]. It has been shown recently that a subset of entangled networks, which we call tanglemers, exhibit high toughness and high fatigue threshold, while maintaining modulus[12–16]. To achieve high toughness and high fatigue threshold, crosslink density should be as low as possible. The lower limit of crosslink density is set by the integrity of the network. To maintain modulus, crosslink density is chosen in the range in which the modulus plateaus as crosslink density changes[12].

Natural rubber from latex has a molecular weight of $M_n \approx 300$ kg mol^{-1}, corresponding to ~4,400 repeat units per chain and ~56 repeat units between neighbouring entanglements[17–20]. Crosslink density C is defined by the molar ratio of crosslinks to the repeat units of the polymer: when $C = 10^{-3}$, the number of repeat units between neighbouring crosslinks is $N = 1/(2C) \approx 500$. In such a network, a strand of polymer between neighbouring crosslinks is much shorter than the polymer chain from the latex, but much longer than a polymer strand between neighbouring entanglements. Our measurements will show that the network falls on the plateau on the curve of modulus as a function of crosslink density. We have also attempted to form networks using an even lower value of C, but the resulting networks have large residual stretch after loading and have substantially lower modulus. By comparison, mastication degrades chains to ~440 repeat units per chain[21]. These relatively short chains necessitate the formation of a network with a high crosslink density of $C \approx 10^{-2}$, corresponding to $N = 1/(2C) \approx 50$ repeat units between neighbouring crosslinks. We will call the network with $C = 10^{-3}$ a tanglemer and the network with $C = 10^{-2}$ a regular natural rubber.

We prepare a natural rubber tanglemer from latex—that is, particles of long polymers dispersed in water. In each particle, polymer chains are ended with non-rubber components, which serve as surfactants to prevent coagulation and as endlinks to network the polymers[5]. We dissolve a small amount of crosslinking agent, dicumyl peroxide (DP), in toluene. Since toluene and water are immiscible, pouring the toluene-DP solution into the latex initially results in two distinct layers (Fig. 2a). After stirring the mixture for six hours, the two layers merge into one, as the polymer particles absorb both toluene and DP (Fig. 2b). We cast the mixture without masticating the polymers. At room temperature, water and toluene evaporate, the polymer particles coalesce into a film and part of the polymers diffuses across the interparticle boundary[22,23]. The film is translucent and the polymers from neighbouring particles are entangled, as well as endlinked through the non-rubber components (Fig. 2c). Entanglements and endlinks between the particles may differ in density from those within individual particles. Subsequently, the film is hot-pressed at 140 °C for three hours, during which the endlinks of the non-rubber components break (Supplementary Fig. 1). During hot-press at 140 °C, several processes take place at various timescales. The endlinks break in a timescale of ~10 min (ref. 24). The reptation time of polymer chains is ~10 min (Supplementary Fig. 2). The half-life for decomposition of DP is ~1 h (ref. 25). Consequently, the first two processes are faster than the last one. Before the polymer chains are crosslinked, polymers have sufficient time to entangle further into neighbouring particles by thermal motion. DP crosslinks polymers into a network (Supplementary Fig. 3), which prevents the polymers from disentangling. As each DP molecule creates a crosslink[25], the crosslink density C is calculated by the molar ratio of DP to the repeat unit of the polymer. The long polymers allow us to use a very low value of C to form a network, called a tanglemer, in which entanglements greatly outnumber crosslinks (Fig. 2d).

Uniaxial tensile behaviour

We form networks with various crosslink densities: $C = 10^{-3}$, 2×10^{-3}, 3.3×10^{-3}, 5×10^{-3} and 10^{-2}. The stress–stretch curve is recorded for each network (Fig. 3a). The average stretchability decreases as C increases (Supplementary Fig. 4). The initial slope of the stress–stretch curve defines modulus E. As C increases, the modulus remains at a plateau of ~1 MPa until $C = 3.3 \times 10^{-3}$, after which the modulus increases mildly (Fig. 3b). The modulus is contributed by both crosslinks and entanglements[10,26,27]:

$$E = \frac{3}{2}\rho k_B T\left(\frac{1}{N} + \frac{1}{N_e}\right) \quad (1)$$

https://doi.org/10.1038/s41893-025-01559-z

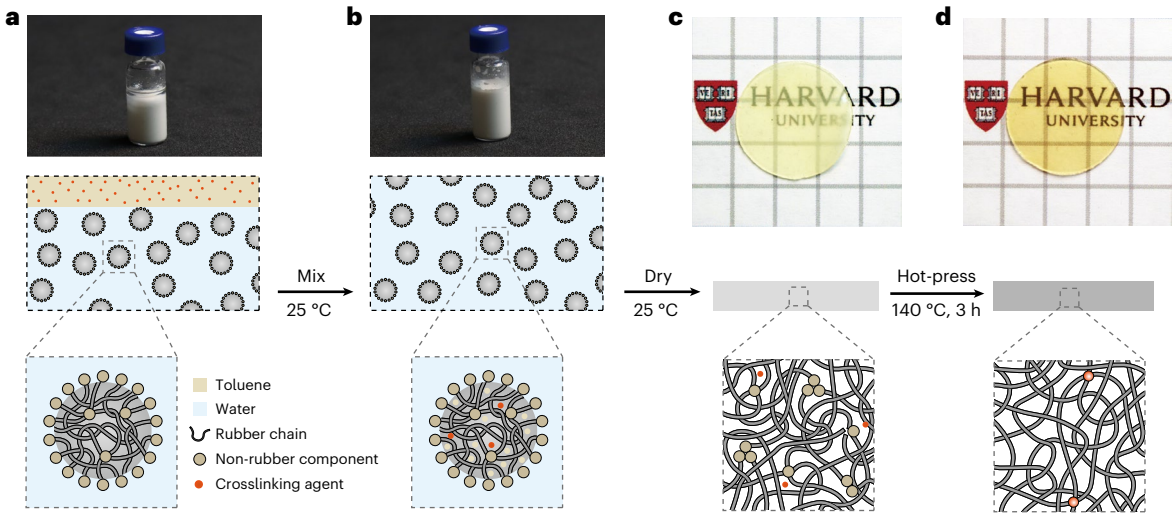

Fig. 2 | Process a latex into a tanglemer. a, Dissolve the crosslinking agent, DP, in toluene and pour the solution into the latex. **b**, Stir to mix the DP solution and the polymer. **c**, Dry the mixture at room temperature to form a film. **d**, Hot-press the film to form a tanglemer.

where ρ is the number of repeating units per unit volume, k_B is the Boltzmann constant, T is the temperature, N_e is the number of repeat units between neighbouring entanglements and N is the number of repeat units between neighbouring crosslinks. For natural rubber, $N_e = 56$ (ref. 22). N can be calculated by $N = 1/(2C)$. When $C = 10^{-3}$, $N = 500$, which is about one order of magnitude larger than N_e. That is, the polymer network is a tanglemer, in which entanglements greatly outnumber crosslinks. As a result, entanglements set the modulus, $E \sim 1/N_e$. This conclusion is further supported by the finding that the plateau modulus of the crosslinked network is approximately the plateau modulus of the melt (Supplementary Fig. 5). As C increases, the effect of crosslinks becomes substantial. When $C = 10^{-2}$, $N = 50$, which is almost the same as N_e, so the modulus exactly doubles the plateau modulus, being 2 MPa.

We load each network to a stretch of two and then unload (Supplementary Fig. 6). For each network, the hysteresis is defined as the ratio of two areas: the area enclosed by the stress–stretch curves of loading and unloading to the area under the stress–stretch curve of loading. All networks have a hysteresis smaller than 20% (Fig. 3c). These low values of hysteresis are comparable to those reported in the literature[28]. At a stretch of two, natural rubber does not undergo SIC and the low hysteresis reflects the low friction between the chains. This conclusion is further corroborated by the dynamic mechanical analysis (Supplementary Fig. 5), where a low tanδ is observed. We also examine creep and recovery of natural rubbers of various crosslink densities. By applying a constant load, the sample mildly elongates over time (Fig. 3d). As the crosslink density decreases, the rate of creep increases. This trend is consistent with previous reports[29,30]. After removing the load, all the networks recover over time (Fig. 3e) and show very small residual strain (<2%, Fig. 3f). In the previous reports, the chains were masticated during processing. Here we preserve the long chains without mastication, and form networks with lower crosslink densities than previously reported. Preserving long polymers expands the range of crosslink density, thereby maximizing performance in applications where both creep resistance and crack resistance are crucial.

We load and unload the tanglemer ($C = 10^{-3}$) and the regular network ($C = 10^{-2}$) at various amplitudes of stretch (Supplementary Fig. 7). For both networks, the hysteresis suddenly increases when the stretch amplitude exceeds ~4 (Fig. 3g), while the residual stretches remain negligible. The amplified hysteresis of natural rubber at large stretches has been attributed to SIC[28]. Additionally, in the nominal stress–stretch curves, both networks soften at stretch ~4–5, and then stiffen as the stretch further increases (Supplementary Fig. 8a). This strain-softening has been ascribed to growth of crystals that reduce the tension and subsequent strain-stiffening occurs because the crystals act as additional crosslinks[28,31]. In the true stress–stretch curves, no strain-softening is observed (Supplementary Fig. 8b).

This inference is supported by wide-angle X-ray scattering (WAXS) observations. In the two-dimensional (2D) WAXS images (Fig. 3h,i), both networks exhibit isotropic halos at low stretches (<2.5), which indicates that the networks are amorphous. As the stretch increases to ~4, both networks show crystal diffraction arcs. Upon further stretch, the crystal diffraction arcs become more pronounced. The 2D WAXS images are converted into 1D intensity profiles[32] (Fig. 3j,k and Supplementary Fig. 9). The tanglemer achieves a much higher maximum crystallinity than that of the regular network (Fig. 3l).

SIC occurs when network strands are stretched to alignment. At each point of entanglement or crosslink, SIC cannot occur. Entanglements within the polymer network can redistribute stress by sliding along strands, unlike crosslinks which restrict movement. Tanglemer exhibits greater stretchability compared to the regular network, enabling it to achieve a higher maximum crystallinity. This effect is consistent with the trend that lower crosslink density enhances crystallinity[33,34]. We examine the crystallinity of networks with various C (Supplementary Fig. 10). As the crosslink density decreases, the maximum crystallinity increases and plateaus, which indicates that the maximum crystallinity is probably set by the entanglement density. Incidentally, the crystallinity of SIC in a poly(ethylene glycol) network increases on removal of entanglements[32]. For the natural rubber reported here, we deliberately retain dense entanglements, so that the modulus remains high. Our data show that, even with dense entanglements, long polymers still amplify the crystallinity of SIC in natural rubber.

Crack resistance under cyclic load

Many applications of natural rubber are limited by crack growth under cyclic load[35]. An amplitude of energy release rate exists, known as the fatigue threshold, below which a crack does not grow. In a polymer strand that bridges a crack, high stress is deconcentrated along the entire strand up to the crosslinks (Fig. 4a). When the polymer strand ruptures at a single covalent bond, the high stress in the entire strand between two crosslinks is relaxed. This molecular picture, proposed by Lake and Thomas[7], leads to the scaling $G_{th} \sim C^{-0.5}$. This Lake–Thomas scaling has long been confirmed in regular rubbers[36,37]. Recently, it has been shown that while crosslinks limit the extent of stress deconcentration,

https://doi.org/10.1038/s41893-025-01559-z

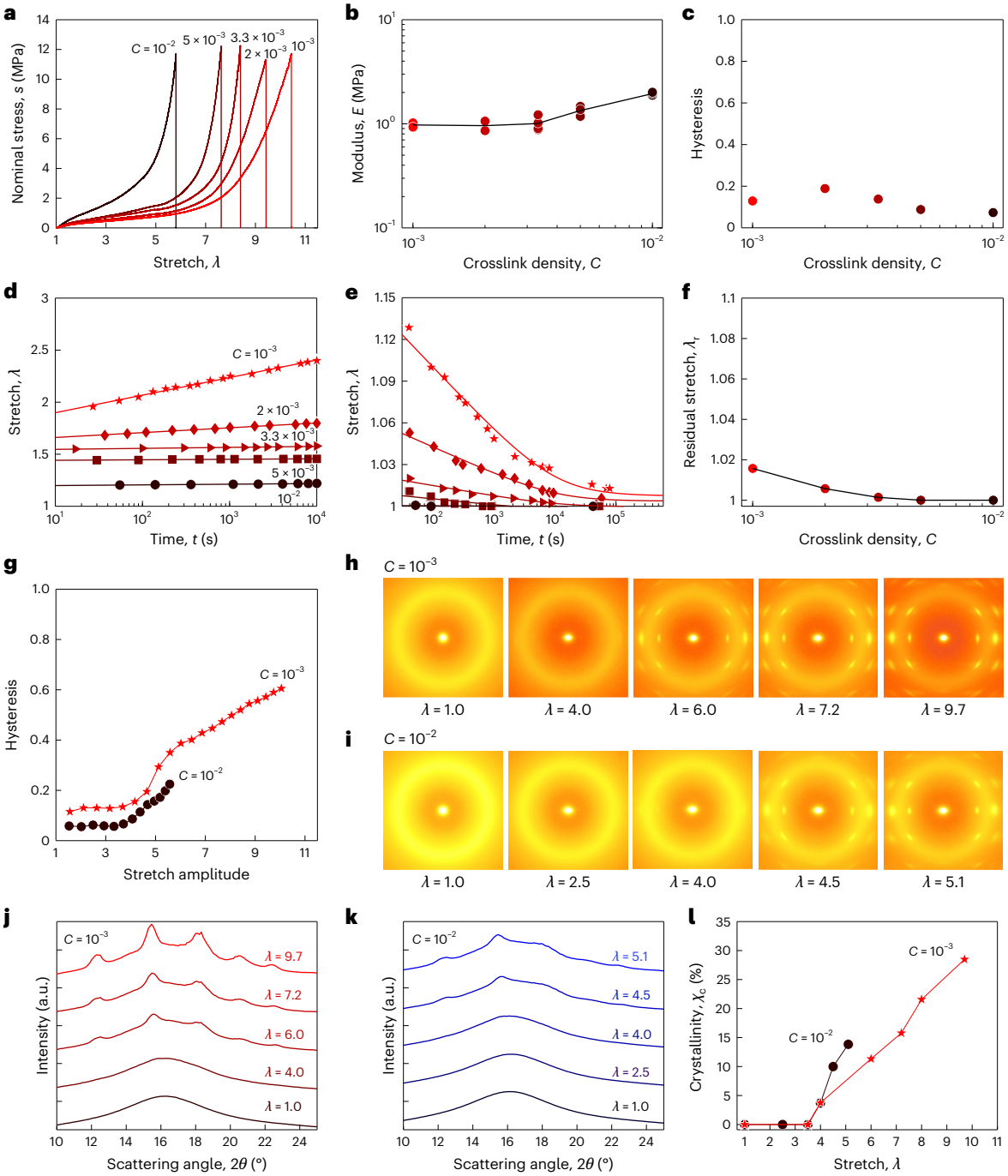

Fig. 3 | Uniaxial tensile behaviour. a, Stress–stretch curves of networks with various crosslink densities, C. **b**, Modulus, E, as a function of C. **c**, Hysteresis as a function of C, measured at a stretch of two. **d**–**f**, Apply 300 kPa to each sample within 1 s, keep for 10^4 s, and then release, all at 25 °C. Creep (**d**) and recovery (**e**) for various values of C. Residual stretch, λ_r, as a function of C, measured 12 h after the load is removed (**f**). **g**, Hysteresis from load–unload curves at various amplitudes of stretch for $C = 10^{-3}$ and 10^{-2}. **h**,**i**, 2D WAXS patterns for $C = 10^{-3}$ (**h**) and $C = 10^{-2}$ (**i**) under various stretches. **j**,**k**,1D WAXS intensity profiles showing crystalline peaks for natural rubber at different stretches: $C = 10^{-3}$ (**j**) and $C = 10^{-2}$ (**k**). **l**, Crystallinity, χ_c, as a function of stretch, λ.

entanglements do not[12–15]. At a crosslink, the highly stressed polymer strand is covalently bonded to multiple other polymer strands. These other polymer strands carry lower stress than the strand that bridges the crack. By contrast, because the frictional stress between polymer strands is much lower than the strength of the covalent bonds along a polymer strand, an entanglement slips, transmitting the high stress in the polymer strand undiminished. For a tanglemer, where entanglements greatly outnumber crosslinks, the dense entanglements do not reduce the fatigue threshold; rather, the fatigue threshold remains limited by crosslink density. We test this theoretical prediction as follows.

For each sample, we measure the crack growth per cycle, dc/dn, as a function of the amplitude of energy release rate, G (Fig. 4b). The amplitude of G is calculated after cyclically loading the sample until the stress–stretch curve reaches a steady state. In our experiments, the minimum crack growth per cycle, dc/dn, that we can detect is ~0.1 nm cycle^{-1}. The linear regression of data estimates the fatigue threshold, G_{th}. The natural rubber tanglemer, $C = 10^{-3}$, achieves a high fatigue threshold of ~200 J m^{-2}, whereas the regular natural rubber, $C = 10^{-2}$, shows a fatigue threshold of ~50 J m^{-2}. At a particular amplitude of energy release rate, for example, $G = 300$ J m^{-2}, the crack growth is

https://doi.org/10.1038/s41893-025-01559-z

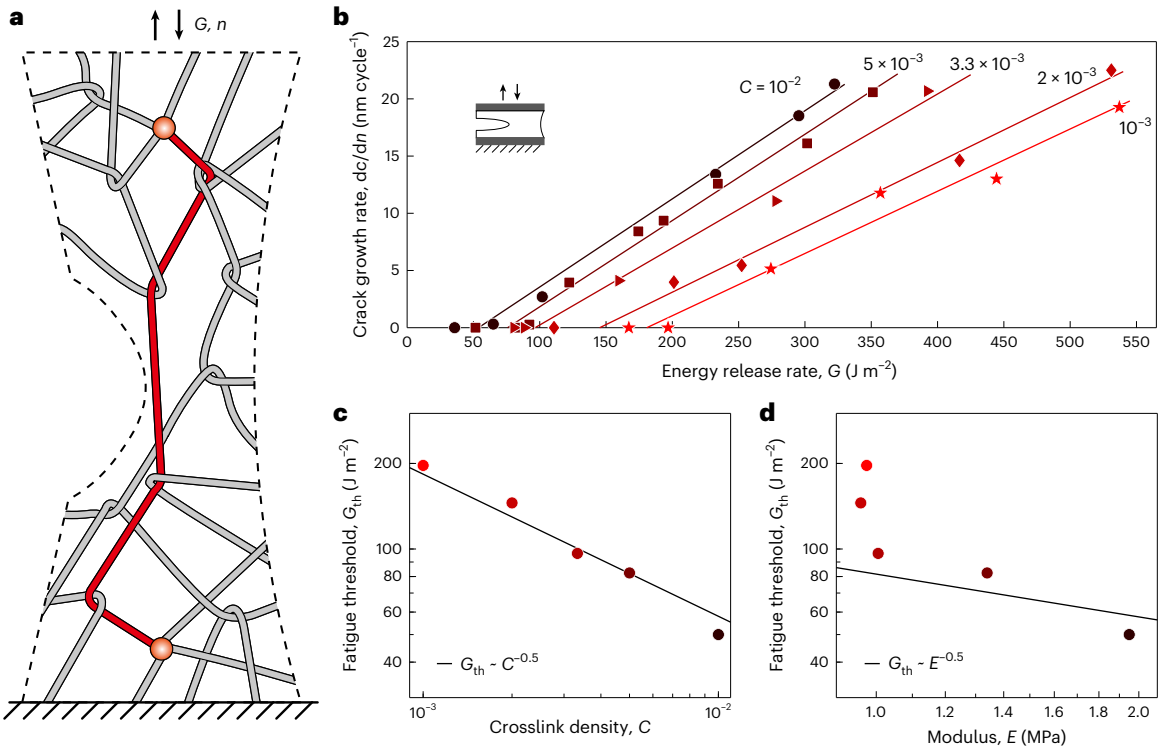

Fig. 4 | Crack growth under cyclic stretch. a, Long polymer strands between neighbouring crosslinks deconcentrate stress. **b**, Crack growth per cycle dc/dn as a function of the amplitude of energy release rate G for networks with various crosslink densities C. **c**, Fatigue threshold G_{th} as a function of C. **d**, Fatigue threshold G_{th} as a function of modulus E.

20 nm cycle^{-1} for a network of $C = 10^{-2}$, and 6 nm cycle^{-1} for a network of $C = 10^{-3}$.

Our experimental data on the fatigue threshold as a function of crosslink density approximately follows the Lake–Thomas scaling (Fig. 4c). For tanglemers, where entanglements greatly outnumber crosslinks, this finding confirms that the crosslinks limit the extent of stress deconcentration, but the entanglements do not. Previous papers have reported that SIC occurs in a region around the crack tip during cyclic loading[38,39]. However, it has been found that SIC does not correlate with the rate at which a crack propagates in fatigue[39]. These findings are consistent with our finding that SIC does not amplify fatigue threshold.

We further plot the fatigue threshold G_{th} as a function of modulus E (Fig. 4d). For a regular network, the modulus scales with crosslink density as $E \sim 1/N \sim C$, and the fatigue threshold scales with modulus as $G_{th} \sim E^{-0.5}$. This trade-off is called modulus-threshold conflict. By contrast, for the tanglemer, the modulus is set by entanglements, $E \sim 1/N_e$, but the threshold still scales with crosslink density, $G_{th} \sim C^{-0.5}$. Consequently, tanglemers overcome the modulus-threshold conflict. As crosslink density decreases, the modulus remains constant while fatigue threshold increases.

Crack resistance under monotonic load

The natural rubber tanglemer greatly amplifies crack resistance (Fig. 5). For a sample with a height of 50 mm and a precrack of 75 mm, the tanglemer does not break at a stretch of 6.04 (Fig. 5a and Supplementary Video 1), but the regular network breaks at a stretch of 1.33 (Fig. 5b and Supplementary Video 2). During stretching, the precrack blunts and bifurcates more in the tanglemer than in the regular network. Imaging under polarized light shows that stress at a crack tip is less concentrated in a tanglemer than in a regular network (Supplementary Video 3).

The crack growth, Δc, is measured as a function of energy release rate, G (Fig. 5c and Supplementary Fig. 11). For the network of a given crosslink density C, we identify two values of energy release rate, G_i and G_c. When $G < G_i$, the crack growth is not observed. When $G_i < G < G_c$, the crack is observed to grow stably with a speed comparable to the velocity of the crosshead of the tensile tester, and the crack arrests when the crosshead stops. When $G = G_c$, the crack grows across the entire sample at a velocity much larger than the velocity of the crosshead. The energy release rate G_i below which crack growth is not observed defines the threshold of crack growth under monotonic stretch. The energy release rate G_c at which the crack grows unstably defines the toughness (Supplementary Fig. 12). The crack growth at which the crack becomes unstable is denoted by Δc_s. As the crosslink density decreases, the threshold, toughness and limit stable crack growth increase. For the tanglemer, $G_i \approx 10$ kJ m^{-2}, $G_c \approx 150$ kJ m^{-2} and $\Delta c_s \approx 2$ mm. For the regular network, $G_i \approx 0.4$ kJ m^{-2}, $G_c \approx 3$ kJ m^{-2} and $\Delta c_s \approx 0.2$ mm.

The above experimental observations may be interpreted as follows (Fig. 5d). Around the crack tip, the polymer strands stretch to alignment and crystallize to form a SIC zone. As stretch increases, the crack grows stably and the SIC zone enlarges. Behind the crack tip, the polymer strands relax the tension, the crystals melt and the network becomes rubbery again. The hysteresis of crystallization and melting dissipates energy. Directly ahead of the crack, the network is bridged by a combination of rubbery strands and crystalline domains. In a crystalline domain, the physical interactions between strands are much weaker than the covalent bonds along individual strands. Consequently, the strands in a crystalline domain slip relative to each other, which delocalizes high tension throughout the crystalline domain. Furthermore, adjacent crystalline domains are separated by thin rubbery strands, so that high tension can spread over multiple crystalline domains.

Crack resistance results from a synergy of two processes: the hysteresis of crystallization and melting in the SIC zone around the crack tip, and the bridging by the strands and crystalline domains ahead of the crack tip. Compared to a regular network, the tanglemer

https://doi.org/10.1038/s41893-025-01559-z

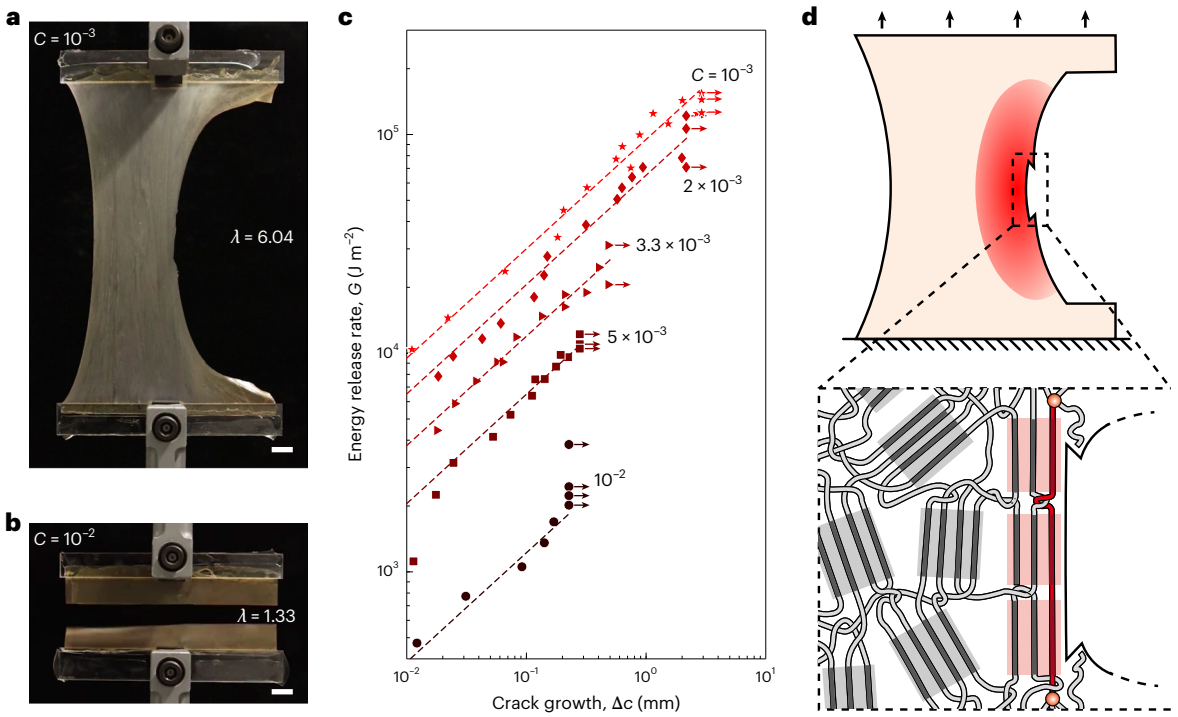

Fig. 5 | Crack growth under monotonic stretch. a,**b**, Stretching a precracked sample of tanglemer ($C = 10^{-3}$) (**a**) and regular network ($C = 10^{-2}$) (**b**). The scale bars represent 20 mm. **c**, The relation between crack growth Δc and energy release rate G for samples of various values of crosslink density C. The solid data points represent stable crack growth and the solid data points with arrows represent unstable crack growth. The starting point of each arrow is an estimate of the limit of stable crack growth, Δc_s. **d**, Strands at the crack tip stretch to alignment and form crystals. When a strand breaks at a single covalent bond, the two parts of the strand release the tension and melt from the crystal, and the crack advances.

has unusually long polymer strands between neighbouring crosslinks. The tanglemer increases the crystallinity, volume of the SIC zone and extent of stress deconcentration of strands and crystalline domains that bridge the crack. These effects synergize to amplify the threshold G_i, toughness G_c and limit stable crack growth Δc_s.

For each network, the fatigue threshold G_{th} measured under cyclic stretch is much lower than the threshold G_i measured under monotonic stretch. The difference between G_{th} and G_i is probably due to two factors. First, the crack growth is observed with a large difference in resolution between the two types of experiments. Under cyclic stretch, our experiment resolves a crack growth of ~0.1 nm cycle^{-1}, whereas under monotonic stretch, our experiment resolves a crack growth of ~20 µm. Second, the crystalline domains directly ahead of the crack tip may play the role of hard particles, which contribute to G_i. However, it has long been established that SIC does not affect G_{th} because these crystalline domains melt after unloading[7,40].

The crack growth as a function of energy release rate was introduced in the classic paper by Thomas[41], and has been called the crack resistance curve, commonly measured in tough materials such as metals and composites[42,43]. Crack resistance curves are rarely reported for elastomers, possibly because the crack growth needed to attain G_c is small for most elastomers. Here we report the crack resistance curve for the natural rubber tanglemer because Δc_s is long.

Crack resistance in extreme conditions

Rubber products are often used under tension. During use, rubbers inevitably contact hard materials. A sharp hard material, contacting a stretched rubber, often causes catastrophic failure. Here we demonstrate that a highly stretched natural rubber tanglemer exhibits an excellent resistance against crack growth in such an extreme case. We compare the natural rubber tanglemer with several other types of rubbers. We load each rubber to a stretch of five, hold the stretch, and then cut the rubber at one edge using a blade (Fig. 6a). The cut grows and arrests in the tanglemer (Fig. 6b), but grows through the other types of rubbers (Fig. 6c and Supplementary Video 4). The tanglemer, stretched nine times its initial length, survives after multiple times of cutting (Supplementary Video 5). As another example, carrying a bottle of water of 1 gallon, cut with a blade, the tanglemer arrests the crack and holds the bottle, but the regular natural rubber fractures and lets the bottle fall (Fig. 6d and Supplementary Video 6).

In many applications, such as springs and mountings, rubbers are subjected to cyclic load between a minimum amplitude and a maximum amplitude[44]. For instance, we cyclically stretch a precracked tanglemer between two values of energy release rates, $G_{min} = 10{,}000$ J m^{-2} and $G_{max} = 12{,}500$ J m^{-2} (Fig. 6e). The precrack in the natural rubber tanglemer does not grow after 50,000 cycles. This superior fatigue resistance can be attributed to the aligned crystalline domain structure ahead of the crack tip[45]. Some of the crystals do not melt because the material is always subject to tension during cyclic loading. Such an effect of permanent tension has been well documented[45,46]. The effect is further amplified by long strands in a tanglemer. The value of G_{max} of 12,500 J m^{-2} exceeds the toughness of the regular natural rubber. That is, the regular natural rubber with a precrack cannot survive from a single cycle of such a load.

Discussion

This work demonstrates that reimagining processes of existing materials can enhance their sustainability. Natural rubber is long known to have a fatigue threshold of ~40 J m^{-2} and a toughness of ~10^4 J m^{-2}. This paper demonstrates that processing the natural rubber latex, without mastication but with dense entanglements and sparse crosslinks, greatly expands the property space of natural rubber. The fatigue threshold is amplified to ~200 J m^{-2} and the toughness is amplified to over 10^5 J m^{-2}.

https://doi.org/10.1038/s41893-025-01559-z

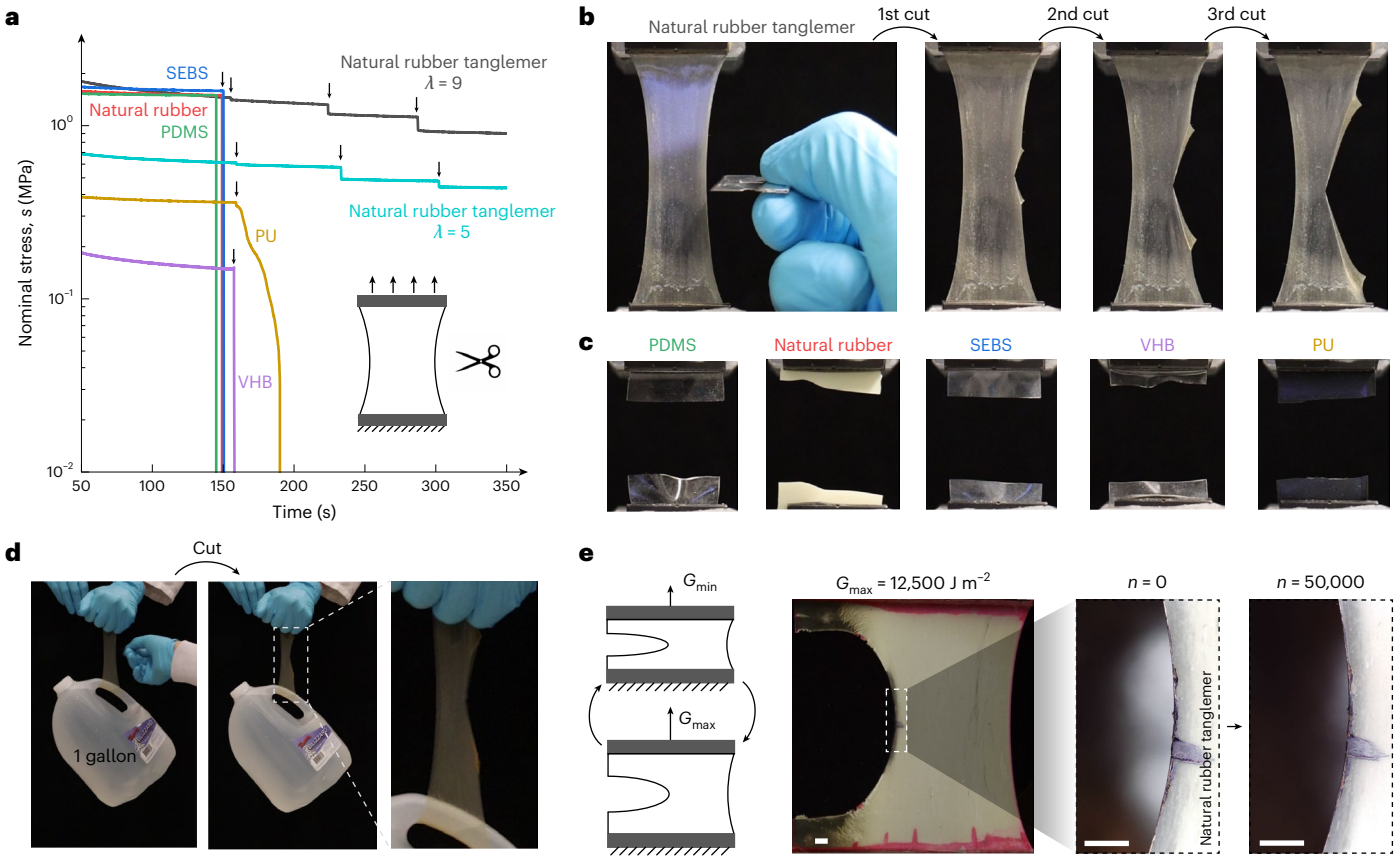

Fig. 6 | Natural rubber tanglemer is crack-resistant in extreme conditions. **a**, Various rubbers are stretched, the stretch is held, and they are cut using a blade. Each arrow on the curve represents a cut. **b**, Photos of natural rubber tanglemer after stretching, holding and cutting. The sample is held at a stretch of nine. The sample survives after three cuts. **c**, Photos of several other types of rubber after stretching, holding and cutting. **d**, The natural rubber tanglemer is hung with a bottle of water of 1 gallon and still bears the load after cutting. **e**, A precracked tanglemer is cyclically loaded between two values of energy release rate G_{min} and G_{max}. After cycles of $n = 50{,}000$ between $G_{min} = 10{,}000\ J\ m^{-2}$ and $G_{max} = 12{,}500\ J\ m^{-2}$, the crack does not grow. The scale bars are 2 mm.

To demonstrate the principle, here we use DP as the crosslinker. DP acts as a crosslinker without activator and accelerator, and is readily mixed with long polymers in the latex. Using DP as a crosslinker has been reported in research papers and patents by the rubber industry, owing to its simplicity, lower compression set and improved heat resistance[47–49]. We should also note that other crosslinking systems are used for natural rubber, such as sulfur and other peroxides. In particular, the majority of natural rubber products so far have been manufactured using the sulfur crosslinking system[47,50]. It has been shown that, for a given crosslink density, natural rubber crosslinked by sulfur is more fatigue resistant than that by DP[51,52]. A thorough study using the sulfur crosslinking system will be important.

The natural rubber tanglemer holds promise in extending the durability of rubber products such as gloves and condoms[53,54]. In load-bearing rubber products, such as tyres, belts and hoses, natural rubbers are reinforced with hard particles[55–57]. It has been demonstrated that particle-reinforced tanglemers have exceptionally high fatigue threshold[15,16]. In these demonstrations, however, tanglemer matrices have been synthesized from monomers, in situ. Natural rubber latex comes with long polymers. Mixing the long polymers with the hard particles is commonly conducted in a high-intensity process using an internal mixer or roll mill, where long polymers are masticated. The current work highlights the potential of maintaining long polymer chains to greatly enhance the crack resistance. Reimagining the mixing method to preserve the long polymer chains is a important challenge to address and remains an open area, which may open a door to extend the lifetime of the particle-reinforced rubber products and reduce rubber pollution.

Methods

Materials

Natural rubber latex with a solid content of 60% by weight was purchased from Chemionics Corporation (OH, US). Dicumyl peroxide (DP, 329541) and toluene (244511) were purchased from Sigma-Aldrich. PDMS was made of Sylgard 184 (Dow Corning) and the mass ratio of the base and the curing agent is 15:1. Commercial natural rubber (8611K16), polyurethane (PU, 8514K311) and polytetrafluoroethylene (PTFE, 8569K23) film were purchased from McMaster-Carr. Styrene-ethylene-butylene-styrene (SEBS, G1657M) was purchased from Kraton. The elastomer sheet of SEBS was fabricated by casting the toluene solution of SEBS.

Natural rubber preparation

DP is dissolved in toluene. Water is added to the natural rubber latex to dilute it to a solid content of 30 wt%. Subsequently, the DP solution is added into the diluted natural rubber latex and the mixture is stirred for 6 h. After stirring, the mixture is rested for 1 h. During mixing and resting, the DP solution gradually absorbs into the latex particles. Dilution of latex avoids coagulation when mixed with the DP solution. The mixture is poured into a glass mould and dried at room temperature for 1 d to form a film. The film is then crosslinked in a hot-press at 140 °C for 3 h, using a PTFE film with a thickness of ~0.5 mm as a spacer. As each DP molecule creates a crosslink[25], the crosslink density C is calculated as the molar ratio of DP to the repeating unit of the polymer. The quantities of DP used to prepare natural rubbers are calculated from C as $m_{DP} = m_{NR}/M_{isoprene} \times C \times M_{DP}$, where m_{DP} is the mass

of DP, m_{NR} is the mass of natural rubber, $M_{isoprene}$ is the molecular weight of a repeating unit of natural rubber chain and M_{DP} is the molecular weight of DP. In particular, the quantity of DP is 0.40 phr, 0.79 phr, 1.31 phr, 1.98 phr and 3.97 phr for $C = 10^{-3}$, 2×10^{-3}, 3.3×10^{-3}, 5×10^{-3} and 10^{-2}, respectively. The unit phr represents the parts per hundred of rubber. For natural rubbers of various crosslink densities, we vary the concentration of the DP solution, so that the mass ratio of the DP solution to the diluted latex is fixed at 1:40.

Rheological test

The dynamic moduli and tanδ of natural rubber are measured using a rheometer (DHR-3, TA Instruments). Natural rubber is cut into samples with a diameter of 20 mm and a thickness of ~0.5 mm. A flat steel plate of the same diameter is adopted. Before each test, the sample is held under compression of ~20 N for 10 min to ensure good contact between the sample and the plate. The samples are measured over a range of oscillation frequencies at a constant oscillation amplitude of 0.2% and at room temperature.

WAXS

WAXS measurements are performed using the Xeuss 3.0 system (Xenocs, France), equipped with a Excillum MetalJet X-ray source of a wavelength of 0.135 nm and a Dectris EIGER2 Si 1 M detector. The experiments are conducted in a transmission mode with sample-to-detector distance of 0.0425 m. The exposure time is about 10 min. The samples are stretched and then held on a rigid frame using clamps. For each crosslink density, samples are measured at various stretches from the initial state to the maximum stretch. Using FIT2D software, 2D WAXS images are converted into 1D intensity profiles by averaging over all azimuthal angles. To determine the crystallinity, background contributions are subtracted and the 1D intensity profiles are deconvoluted into amorphous and crystalline peaks using a Gaussian function. The crystallinity is estimated by $\chi_c = A_c/(A_c + A_a)$, where A_c and A_a represent the total integrated area of fitted crystalline and amorphous peaks, respectively.

Mechanical tests

Stress–stretch curves are measured by uniaxial tension tests. We cut the natural rubber sheet into dogbone-shaped samples. The gauge section of each sample has a dimension of 10 × 2 × 0.5 (length × width × thickness, mm). Deformation at the gauge section of the sample is homogeneous. We measure the displacement at the gauge section by marking two points to calculate the stretch. Each sample is stretched under a fixed loading rate of ~0.01 s^{-1} until rupture. We load and unload the dogbone-shaped samples and calculate hysteresis as the ratio of two areas: the area enclosed by the stress–stretch curves of loading and unloading, and the area under the stress–stretch curve of loading.

The crack growth under cyclic load and fatigue threshold are measured by using pure shear samples. We prepare two samples, with and without a precrack. Both samples have the same dimension of 50 × 10 × 0.5 (width × height × thickness, mm). For the precracked sample, the initial crack length is 15 mm. We first load and unload the sample without a precrack for 500 cycles at an amplitude of stretch λ. During cyclic loading, the stress–stretch curve exhibits shakedown and reaches a steady state. We then calculate strain energy per unit volume $W(\lambda)$ from the area under the stress–stretch curve at the steady state[58,59]. We cyclically load and unload the sample with a precrack at a frequency of ~1.0 Hz. For each measurement, we prescribe the amplitude of stretch λ, and the amplitude of energy release rate is calculated as $G = W(\lambda)H$, where H is the height of the sample in the undeformed state. The crack growth per cycle, dc/dn, is obtained by dividing the crack growth by the number of cycles. Between 10,000 and 200,000 cycles are performed for each measurement. The crack growth is observed under an optical microscope with a resolution of ~20 μm. The fatigue threshold is determined after 200,000 cycles of load and unload if we cannot detect any crack growth. Based on these conditions, the minimum crack growth that we can detect is ~0.1 nm $cycle^{-1}$.

The toughness is measured by the pure shear test. We prepare two samples, with and without a precrack. The sample dimension is 200 × 50 × 0.5 (width × height × thickness, mm). For the precracked sample, the precrack is introduced by using a blade and is 75 mm long. Both samples are stretched at a fixed loading rate of 0.01 s^{-1}. From the sample without a precrack, we obtain strain energy per unit volume as a function of the stretch, $W(\lambda)$. From the sample with a precrack, we measure the critical stretch λ_c, at which the precrack suddenly grows and fractures the entire sample. We then calculate the toughness, $G_c = W(\lambda_c)H$.

Similar to measuring the toughness, we measure the crack growth under monotonic load using the pure shear test. Before loading a sample, we make a precrack in the sample and take an image focusing on the crack tip by using a microscope. We load the sample to a stretch smaller than the critical stretch, $\lambda < \lambda_c$, and hold the sample for a short time to make sure the crack is arrested. We then unload the sample and take another image focusing on the crack tip. By comparing the crack tip before and after load, we determine the crack growth Δc at the prescribed stretch λ. The prescribed stretch can be converted to an energy release rate by $G = W(\lambda)H$. For each measurement, we make a fresh precrack, load the sample to a prescribed stretch, unload the sample, and measure the crack growth.

All the mechanical tests are performed using a tensile tester (Instron 5966), except that the fatigue fracture test is performed using an in-house developed tester.

Reporting summary

Further information on research design is available in the Nature Portfolio Reporting Summary linked to this article.

Data availability

All data presented in the Supplementary Information figures are available as Source Data. Source data are provided with this paper.

References

1. Watari, T., Hata, S., Nakajima, K. & Nansai, K. Limited quantity and quality of steel supply in a zero-emission future. *Nat. Sustain.* **6**, 336–343 (2023).
2. Del Rio, D. D. F. et al. Decarbonizing the glass industry: a critical and systematic review of developments, sociotechnical systems and policy options. *Renew. Sustain. Energy Rev.* **155**, 111885 (2022).
3. Wu, W. et al. Reprocessable and ultratough epoxy thermosetting plastic. *Nat. Sustain.* **7**, 804–811 (2024).
4. Assi, L. et al. Sustainable concrete: building a greener future. *J. Clean. Prod.* **198**, 1641–1651 (2018).
5. Tanaka, Y. & Tarachiwin, L. Recent advances in structural characterization of natural rubber. *Rubber Chem. Technol.* **82**, 283–314 (2009).
6. White, J. L. in *Science and Technology of Rubber* 2nd edn (eds Mark, J. E. et al.) 257–338 (Elsevier, 1994).
7. Lake, G. J. & Thomas, A. G. The strength of highly elastic materials. *Proc. R. Soc. A* **300**, 108–119 (1967).
8. Rivlin, R. S. & Thomas, A. G. Rupture of rubber. I. Characteristic energy for tearing. *J. Polym. Sci.* **10**, 291–318 (1953).
9. de Gennes, P. G. Reptation of a polymer chain in the presence of fixed obstacles. *J. Chem. Phys.* **55**, 572–579 (1971).
10. Patel, S. K., Malone, S., Cohen, C., Gillmor, J. R. & Colby, R. H. Elastic modulus and equilibrium swelling of poly(dimethylsiloxane) networks. *Macromolecules* **25**, 5241–5251 (1992).
11. Rubinstein, M. & Panyukov, S. Elasticity of polymer networks. *Macromolecules* **35**, 6670–6686 (2002).
12. Kim, J., Zhang, G., Shi, M. & Suo, Z. Fracture, fatigue, and friction of polymers in which entanglements greatly outnumber cross-links. *Science* **374**, 212–216 (2021).

13. Nian, G., Kim, J., Bao, X. & Suo, Z. Making highly elastic and tough hydrogels from doughs. *Adv. Mater.* **34**, 2206577 (2022).
14. Bao, X. et al. Low-intensity mixing process of high molecular weight polymer chains leads to elastomers of long network strands and high fatigue threshold. *Soft Matter* **19**, 5956–5966 (2023).
15. Steck, J., Kim, J., Kutsovsky, Y. & Suo, Z. Multiscale stress deconcentration amplifies fatigue resistance of rubber. *Nature* **624**, 303–308 (2023).
16. Chen, Z., Zhang, G., Luo, Y. & Suo, Z. Rubber-glass nanocomposites fabricated using mixed emulsions. *Proc. Natl Acad. Sci. USA* **121**, e2322684121 (2024).
17. Westall, B. The molecular weight distribution of natural rubber latex. *Polymer* **9**, 243–248 (1968).
18. Fuller, K. N. G. & Fulton, W. S. The influence of molecular weight distribution and branching on the relaxation behaviour of uncrosslinked natural rubber. *Polymer* **31**, 609–615 (1990).
19. Tangpakdee, J. & Tanaka, Y. Characterization of sol and gel in *Hevea* natural rubber. *Rubber Chem. Technol.* **70**, 707–713 (1997).
20. Fetters, L. J., Lohse, D. J., Richter, D., Witten, T. A. & Zirkel, A. Connection between polymer molecular weight, density, chain dimensions, and melt viscoelastic properties. *Macromolecules* **27**, 4639–4647 (1994).
21. Harmon, D. J. & Jacobs, H. L. Degradation of natural rubber during mill mastication. *J. Appl. Polym. Sci.* **10**, 253–257 (1966).
22. Winnik, M. A. Latex film formation. *Curr. Opin. Colloid Interface Sci.* **2**, 192–199 (1997).
23. Wei, Y.-C., Xia, J.-H., Zhang, L., Zheng, T.-T. & Liao, S. Influence of non-rubber components on film formation behavior of natural rubber latex. *Colloid Polym. Sci.* **298**, 1263–1271 (2020).
24. Amnuaypornsri, S., Sakdapipanich, J. & Tanaka, Y. Green strength of natural rubber: the origin of the stress–strain behavior of natural rubber. *J. Appl. Polym. Sci.* **111**, 2127–2133 (2009).
25. Thomas, D. K. Crosslinking efficiency of dicumyl peroxide in natural rubber. *J. Appl. Polym. Sci.* **6**, 613–616 (1962).
26. Flory, P. J. *Principles of Polymer Chemistry* (Cornell Univ. Press, 1953).
27. Rubinstein, M. & Colby, R. H. *Polymer Physics* (Oxford Univ. Press, 2003).
28. Trabelsi, S., Albouy, P.-A. & Rault, J. Crystallization and melting processes in vulcanized stretched natural rubber. *Macromolecules* **36**, 7624–7639 (2003).
29. Plazek, D. J. Effect of crosslink density on the creep behavior of natural rubber vulcanizates. *J. Polym. Sci. A2 Polym. Phys.* **4**, 745–763 (1966).
30. Farlie, E. D. Creep and stress relaxation of natural rubber vulcanizates. Part I. Effect of crosslink density on the rate of creep in different vulcanizing systems. *J. Appl. Polym. Sci.* **14**, 1127–1141 (1970).
31. Flory, P. J. Thermodynamics of crystallization in high polymers. I. Crystallization induced by stretching. *J. Chem. Phys.* **15**, 397–408 (1947).
32. Hartquist, C. M. et al. An elastomer with ultrahigh strain-induced crystallization. *Sci. Adv.* **9**, eadj0411 (2023).
33. Chenal, J.-M., Chazeau, L., Guy, L., Bomal, Y. & Gauthier, C. Molecular weight between physical entanglements in natural rubber: a critical parameter during strain-induced crystallization. *Polymer* **48**, 1042–1046 (2007).
34. Huneau, B. Strain-induced crystallization of natural rubber: a review of X-ray diffraction investigations. *Rubber Chem. Technol.* **84**, 425–452 (2011).
35. Mars, W. & Fatemi, A. A literature survey on fatigue analysis approaches for rubber. *Int. J. Fatigue* **24**, 949–961 (2002).
36. Bhowmick, A. K. Threshold fracture of elastomers. *J. Macromol. Sci. C* **28**, 339–370 (1988).
37. Zhou, Y. et al. The stiffness-threshold conflict in polymer networks and a resolution. *J. Appl. Mech.* **87**, 031002 (2020).
38. Rublon, P. et al. In situ synchrotron wide-angle X-ray diffraction investigation of fatigue cracks in natural rubber. *J. Synchrotron Radiat.* **20**, 105–109 (2013).
39. Demassieux, Q., Berghezan, D. & Creton, C. in *Fatigue Crack Growth in Rubber Materials*, Vol. 286 (eds Heinrich, G. et al.) 467–491 (Springer International Publishing, 2020).
40. Lake, G. J. & Lindley, P. B. Cut growth and fatigue of rubbers. II. Experiments on a noncrystallizing rubber. *J. Appl. Polym. Sci.* **8**, 707–721 (1964).
41. Thomas, A. G. Rupture of rubber. V. Cut growth in natural rubber vulcanizates. *J. Polym. Sci.* **31**, 467–480 (1958).
42. Suo, Z., Bao, G. & Fan, B. Delamination R-curve phenomena due to damage. *J. Mech. Phys. Solids* **40**, 1–16 (1992).
43. Launey, M. E. & Ritchie, R. O. On the fracture toughness of advanced materials. *Adv. Mater.* **21**, 2103–2110 (2009).
44. Mars, W. V. & Fatemi, A. Factors that affect the fatigue life of rubber: a literature survey. *Rubber Chem. Technol.* **77**, 391–412 (2004).
45. Saintier, N., Cailletaud, G. & Piques, R. Cyclic loadings and crystallization of natural rubber: an explanation of fatigue crack propagation reinforcement under a positive loading ratio. *Mater. Sci. Eng. A* **528**, 1078–1086 (2011).
46. Lindley, P. B. Relation between hysteresis and the dynamic crack growth resistance of natural rubber. *Int. J. Fract.* **9**, 449–462 (1973).
47. Ikeda, Y., Yasuda, Y., Hijikata, K., Tosaka, M. & Kohjiya, S. Comparative study on strain-induced crystallization behavior of peroxide cross-linked and sulfur cross-linked natural rubber. *Macromolecules* **41**, 5876–5884 (2008).
48. Kruželák, J., Sýkora, R. & Hudec, I. Peroxide vulcanization of natural rubber. Part I: effect of temperature and peroxide concentration. *J. Polym. Eng.* **34**, 617–624 (2014).
49. Parks, C. R. Retardation of scorch in rubber compounds containing dicumyl peroxide as the vulcanizing agent. US Patent 3,384,613 (1968).
50. González Hernández, L., Rodríguez-Díaz, A., Valentín, J. L., Marcos-Fernández, Á. & Posadas, P. Conventional and efficient crosslinking of natural rubber: effect of heterogeneities on the physical properties. *KGK Kautsch. Gummi Kunstst.* **58**, 638–643 (2005).
51. Yanyo, L. C. Effect of crosslink type on the fracture of natural rubber vulcanizates. *Int. J. Fract.* **39**, 103–110 (1989).
52. Cox, W. L. & Parks, C. R. Effect of curing systems on fatigue of natural rubber vulcanizates. *Rubber Chem. Technol.* **39**, 785–797 (1966).
53. Wilkinson, B., Ingram, G. D. & Waumsley, H. Manufacture of rubber in sheet or crepe form and of rubber articles. US Patent 2,358,195 (1944).
54. Rafał Kędzia, J., Maria Sitko, A., Tadeusz Haponiuk, J. & Kucińska Lipka, J. in *Application and Characterization of Rubber Materials* (eds Evingür, G. A. & Pekcan, Ö.) Ch. 5 (InTechOpen, 2022).
55. Gent, A. N. *Engineering with Rubber: How to Design Rubber Components* (Hanser Publishers, 2012).
56. Candau, N., Chazeau, L., Chenal, J.-M., Gauthier, C. & Munch, E. Compared abilities of filled and unfilled natural rubbers to crystallize in a large strain rate domain. *Compos. Sci. Technol.* **108**, 9–15 (2015).
57. Demassieux, Q., Berghezan, D., Cantournet, S., Proudhon, H. & Creton, C. Temperature and aging dependence of strain-induced crystallization and cavitation in highly crosslinked and filled natural rubber. *J. Polym. Sci. B Polym. Phys.* **57**, 780–793 (2019).
58. Creton, C. & Ciccotti, M. Fracture and adhesion of soft materials: a review. *Rep. Prog. Phys.* **79**, 046601 (2016).

59. Bai, R., Yang, J. & Suo, Z. Fatigue of hydrogels. *Eur. J. Mech.* **74**, 337–370 (2019).
60. Fleck, N. A., Kang, K. J. & Ashby, M. F. Overview no. 112: the cyclic properties of engineering materials. *Acta Metall. Mater.* **42**, 365–381 (1994).
61. Li, C., Yang, H., Suo, Z. & Tang, J. Fatigue-resistant elastomers. *J. Mech. Phys. Solids* **134**, 103751 (2020).

Acknowledgements

This work was supported by the National Science Foundation under MRSEC (DMR-2011754). Z.S. acknowledges the support of the Air Force Office of Scientific Research under award number FA9550-20-1-0397. M.W.M.T. gratefully acknowledges the financial support under the College of Engineering International Postdoctoral Fellowship, which is jointly provided by the Ministry of Education, Singapore and Nanyang Technological University, Singapore.

Author contributions

G.N., Z.C. and X.B. conceived the project. G.N., Z.C., X.B. and M.W.M.T. conducted the experiments and analysed the results. Z.S. and Y.K. supervised the research. All the authors designed the study, and wrote and edited the manuscript.

Competing interests

The authors declare no competing interests.

Additional information

Supplementary information The online version contains supplementary material available at https://doi.org/10.1038/s41893-025-01559-z.

Correspondence and requests for materials should be addressed to Zhigang Suo.

Peer review information *Nature Sustainability* thanks Costantino Creton and the other, anonymous, reviewer(s) for their contribution to the peer review of this work.

Reprints and permissions information is available at www.nature.com/reprints.

Publisher's note Springer Nature remains neutral with regard to jurisdictional claims in published maps and institutional affiliations.

Springer Nature or its licensor (e.g. a society or other partner) holds exclusive rights to this article under a publishing agreement with the author(s) or other rightsholder(s); author self-archiving of the accepted manuscript version of this article is solely governed by the terms of such publishing agreement and applicable law.

© The Author(s), under exclusive licence to Springer Nature Limited 2025

nature portfolio

Corresponding author(s): Zhigang Suo

Last updated by author(s): Mar 27, 2025

Reporting Summary

Nature Portfolio wishes to improve the reproducibility of the work that we publish. This form provides structure for consistency and transparency in reporting. For further information on Nature Portfolio policies, see our Editorial Policies and the Editorial Policy Checklist.

Statistics

For all statistical analyses, confirm that the following items are present in the figure legend, table legend, main text, or Methods section.

n/a	Confirmed	
☐	☒	The exact sample size (*n*) for each experimental group/condition, given as a discrete number and unit of measurement
☐	☒	A statement on whether measurements were taken from distinct samples or whether the same sample was measured repeatedly
☒	☐	The statistical test(s) used AND whether they are one- or two-sided *Only common tests should be described solely by name; describe more complex techniques in the Methods section.*
☐	☒	A description of all covariates tested
☐	☒	A description of any assumptions or corrections, such as tests of normality and adjustment for multiple comparisons
☐	☒	A full description of the statistical parameters including central tendency (e.g. means) or other basic estimates (e.g. regression coefficient) AND variation (e.g. standard deviation) or associated estimates of uncertainty (e.g. confidence intervals)
☒	☐	For null hypothesis testing, the test statistic (e.g. *F*, *t*, *r*) with confidence intervals, effect sizes, degrees of freedom and *P* value noted *Give P values as exact values whenever suitable.*
☒	☐	For Bayesian analysis, information on the choice of priors and Markov chain Monte Carlo settings
☐	☒	For hierarchical and complex designs, identification of the appropriate level for tests and full reporting of outcomes
☒	☐	Estimates of effect sizes (e.g. Cohen's *d*, Pearson's *r*), indicating how they were calculated

Our web collection on statistics for biologists contains articles on many of the points above.

Software and code

Policy information about availability of computer code

Data collection	The data are collected manually.
Data analysis	FIT2D software (version 12.077) is used for WAXS data analysis.

For manuscripts utilizing custom algorithms or software that are central to the research but not yet described in published literature, software must be made available to editors and reviewers. We strongly encourage code deposition in a community repository (e.g. GitHub). See the Nature Portfolio guidelines for submitting code & software for further information.

Data

Policy information about availability of data

All manuscripts must include a data availability statement. This statement should provide the following information, where applicable:

- Accession codes, unique identifiers, or web links for publicly available datasets
- A description of any restrictions on data availability
- For clinical datasets or third party data, please ensure that the statement adheres to our policy

All data presented in the Figures are available as Source Data. All data presented in the Supplementary Figures are available as Supplementary Data.

Human research participants

Policy information about studies involving human research participants and Sex and Gender in Research.

Reporting on sex and gender	N/A
Population characteristics	N/A
Recruitment	N/A
Ethics oversight	N/A

Note that full information on the approval of the study protocol must also be provided in the manuscript.

Field-specific reporting

Please select the one below that is the best fit for your research. If you are not sure, read the appropriate sections before making your selection.

☐ Life sciences ☐ Behavioural & social sciences ☒ Ecological, evolutionary & environmental sciences

For a reference copy of the document with all sections, see nature.com/documents/nr-reporting-summary-flat.pdf

Ecological, evolutionary & environmental sciences study design

All studies must disclose on these points even when the disclosure is negative.

Study description	We process a biopolymer, the natural rubber latex, in to a tanglemer, in which entanglements greatly outnumber crosslinks. The nature rubber tanglemer shows greatly improved properties, which holds promise to extend the lifetimes of established products, and to result in new products. A more durable biopolymer will reduce polymer pollution and enhance sustainability.
Research sample	Natural rubber
Sampling strategy	N/A
Data collection	The data is manually collected
Timing and spatial scale	N/A
Data exclusions	N/A
Reproducibility	See Methods section
Randomization	N/A
Blinding	N/A

Did the study involve field work? ☐ Yes ☒ No

Reporting for specific materials, systems and methods

We require information from authors about some types of materials, experimental systems and methods used in many studies. Here, indicate whether each material, system or method listed is relevant to your study. If you are not sure if a list item applies to your research, read the appropriate section before selecting a response.

Materials & experimental systems

n/a	Involved in the study
☒	☐ Antibodies
☒	☐ Eukaryotic cell lines
☒	☐ Palaeontology and archaeology
☒	☐ Animals and other organisms
☒	☐ Clinical data
☒	☐ Dual use research of concern

Methods

n/a	Involved in the study
☒	☐ ChIP-seq
☒	☐ Flow cytometry
☒	☐ MRI-based neuroimaging